Journal of Nanostructure in Chemistry (2018) 8:103–121
https://doi.org/10.1007/s40097-018-0258-5

ORIGINAL RESEARCH

Preparation and characterization of MWCNT–COOH–cellulose–MgO NP nanocomposite as adsorbent for removal of methylene blue from aqueous solutions: isotherm, thermodynamic and kinetic studies

Mohammad Sajjad Khalili[1] · Karim Zare[1] · Omid Moradi[2] · Mika Sillanpää[3]

Received: 22 January 2018 / Accepted: 8 March 2018 / Published online: 26 March 2018

Abstract
In this work, MWCNT–COOH–cellulose nanocomposite was prepared with MWCNT–COOH, SOCl2 as leaving group and cellulose as an adsorbent (A1); MgO nanoparticles have been successfully coated on the surface of nanocomposite by directly adding to A1 (MWCNT–COOH–cellulose–MgO; A2), magnesium nitrate was added to A1 and MgO nanoparticles were achieved by coating indirectly on the surfaces (MWCNT–COOH–cellulose–MgO; A3). These nanocomposites (A1, A2, and A3) were used for the removal of methyleneblue (MB) dye from aqueous solution. For characterization of adsorbent surfaces, the FT-IR, TEM, SEM, and XRD analysis were used. The effects of initial concentration of MB dye, contact time, and temperature on the adsorption were studied. According to the results, 55 min was selected as the optimum contact time for the removal process. The equilibrium data of adsorption were well fitted and the Langmuir (type III) model had the best agreement because it possesses high value of linear regression, high value R^2, and least value of average relative error, ARE (%). Parameters of thermodynamics including enthalpy (ΔH°), entropy (ΔS°), and Gibbs energy (ΔG°) were calculated. Kinetic data had best agreement with pseudo-second-order model.

Graphical abstract Schematic synthesis of MWCNT–COOH–cellulose–MgO NP nanocomposite as adsorbent

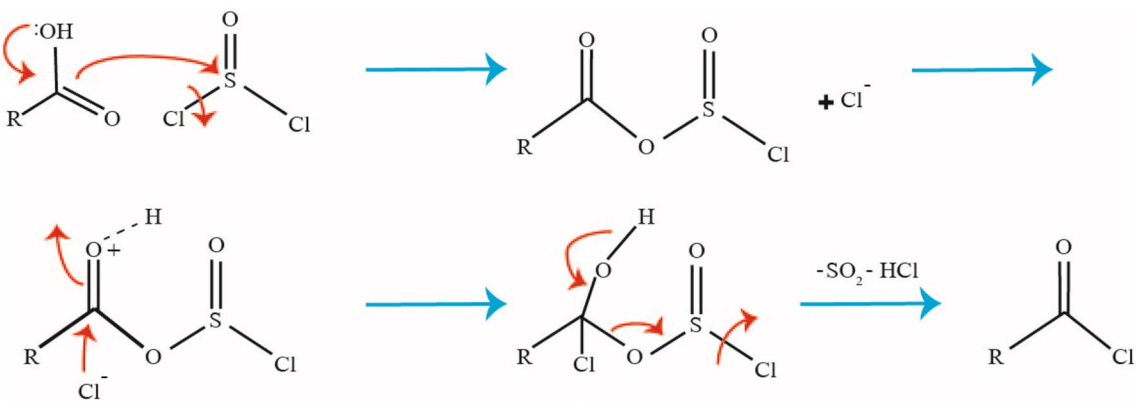

Keywords Methylene blue · Cellulose · Adsorption · MWCNT–COOH; · Nanoparticle of MgO

Introduction

Water pollution caused by different industries such as leather, dye synthesis, food, paper, plastic, textile, cosmetics, and printing has attracted much attention because most of these dyes are harmful to human health and

✉ Karim Zare
k-zare@srbiau.ac.ir; karim_zare84@yahoo.com

Extended author information available on the last page of the article

environment [1]. Therefore, it is necessary to treat dye wastewater. Recently, dye removal from wastewater has become more important [2, 3]. Different methods of treatment such as chemical, physical, and biological have been applied to dye removal from effluent [4, 5].

Adsorption is an effective, easy, and economic method for the removal of industrial dyes [6–8]. Many adsorbents, such as silica, zeolite, orange peel, wheat shells, almond shells, coir pith, and polymeric materials, have been applied and studied [9–12]. Adsorption of water in porous materials has been widely used in many important processes of industry, such as drying of gas and liquid, thermal energy conversion, and storage and humidity control [12].

Nowadays, many studies are being done on natural renewable polymers because of the importance of protecting the environment, the saving energy, and removal of pollution from aqueous solution. In addition, environmentally biodegradable polymers from renewable resources have attracted great attention with expertise in diverse areas. As a renewable source-based biodegradable polymer, cellulose is a kind of thermoplastic material produced by the esterification of naturally abundant cellulose materials such as cotton, wood pulp, sugarcane, and recycled paper.

Methylene blue (MB) dye causes irritation to the eye which may also cause permanent injury to animal and human eyes [13]. In addition, methylene blue dye can give rise to rapid short periods of breathing difficulty, while effective adsorption through mouth produces a burning sensation and can cause vomiting, profuse sweating, methemoglobinemia, painful micturition, mental confusion, and nausea [14, 15]. Therefore, because of the considerable resistance of MB, chemical, biological, and physical methods [16] for methylene blue removal have been widely studied, such as oxidation advance, adsorption, photocatalysis, filtration on membrane, and electrochemical techniques [14–17].

Carbon nanotubes (CNTs) are considered as reinforcement for polymer matrix because of their remarkable electrical, chemical, and physical properties with small dimensions and high ratio aspect [18, 19]. In many articles, nanotubes have been reported as adsorbent due to their special properties [19]. Multi-walled nanotubes (MWNTs) consist of concentric tubes (multiple rolled layers) of graphene. Multi-walled carbon nanotubes have high contact area which increases the adsorbent efficiency due to the presence of multiple walls in comparison to single-walled carbon nanotubes.

Cellulose with the molecular formula $C_6H_{10}O_5$ is an organic polysaccharide consisting of a linear chain of hundreds to thousands of differently linked units of D-glucose. Cellulose is widely used to produce paper and paperboard. Smaller amounts are also converted into a high variety of products of derivative such as rayon and cellophane. Cellulose conversion from energy crop into biofuels such as cellulosic ethanol is under research as another source of fuel. In industry, cellulose use is mainly obtained from cotton and wood pulp [20].

In this work, MWCNT–COOH–cellulose nanocomposite was prepared with MWCNT–COOH, SOCl2 as leaving group and cellulose as an adsorbent (A1), MgO nanoparticles have been successfully coated on the surface of nanocomposite by directly adding to A1, (MWCNT–COOH–cellulose–MgO; A2), magnesium nitrate was added to A1 and MgO nanoparticles were achieved by coating indirectly on the surfaces (MWCNT–COOH–cellulose–MgO; A3). Fourier transform infrared (FT-IR), transmission electron microscopy (TEM), X-ray diffraction (XRD), and scanning electron microscopy (SEM) analyses were used for the characterization of all adsorbent surfaces. The effect of various parameters such as contact time, initial concentration, and temperature on the adsorption capability as well as MB removal capacity of the A1, A2, and A3 as adsorbents was studied in detail. The isotherm, kinetic and thermodynamic parameters, Gibbs energy (ΔG°), entropy (ΔS°), and enthalpy (ΔH°) were calculated. The result shows that the synthesis of A1, A2, and A3 as adsorbents has the potential to remove MB from wastewater.

Experimental

Materials

MWCNT–COOH (extent of labeling: 8% carboxylic acid functionalized, avg. diam. XL: 9.5 nm × 1.5 µm, assay: > 8% carbon basis, functional group: carboxyl), cellulose [particle size: 51 µm, pH 5–7 (11wt%), bulk density: 0.6 g/ml (25 °C)], MgO nanoparticles (particle size > 50 nm), $Mg(NO_3)_2.6H_2O$ [assay: 99.999% trace metals basis, mp: 89 °C (dec.) (lit.)], thionyl chloride [vapor pressure: 97 mmHg (20 °C), assay: ≥ 99%], tetrahydrofuran (THF), methylene blue (assay: > 96.0%), ethylene glycol dimethacrylate [vapor density: > 1 (VS air), vapor pressure: < 0.1 mm Hg (21.1 °C), assay: 98%, bp 98–100 °C/5 mmHg (lit.)], NaOH [assay: > 98% (*T*), vapor density: > 1 (VS air), vapor pressure: 18 mmHg (20 °C)], and urea [concentration: 8 M, solubility: H_2O soluble (1 vial plus 16 mL)] were used in this study and purchased from Sigma-Aldrich Company.

Methods

Preparation of nanocomposite

Nanocomposite-based MWCNT–COOH–cellulose was fabricated as an adsorbent. All solutions were prepared with deionized water (Milli-Q treated). First, Cl group of the $SOCl_2$ was replaced with the OH group in MWCNT–COOH.

For this study, 1 g MWCNT–COOH and 50 ml thionyl chloride were dissolved in 10 ml of tetrahydrofuran (THF). This solution was reflexed for 50 h. Then reaction mixture solution was filtered through 0.22-μm filter with deionized water. MWCNT–COOH–cellulose nanocomposite and 2 g cellulose were successfully dissolved in aqueous NaOH/urea, then 1 g MWCNT–COOH–$SOCl_2$ and 1.5 ml ethylene glycol dimethacrylate (EDGMA) as cross-linking agent were added to solution. This solution was reflexed at 70 °C for 4 h. Then the solution was placed in the ultrasonic bath at a fixed temperature. Ultrasonic bath (71020-DTH-E; model 1510 DTH, 220 V; EMS Company) was used to prevent the aggregation of the particles. Then reaction mixture solution was filtered through a 0.22-μm filter with deionized water. We put it in the oven with operating temperature of 50 °C for 24 h (A1). Then, 0.5 g nanocomposite (A1) and 0.05 g MgO nanoparticle were added to 75 ml water. This solution was reflexed for 3 h at 70 °C and was placed in ultrasonic bath for 2 h. Then reaction mixture was filtered with deionized water. Afterwards, we put it in the oven with operating temperature of 50 °C for 24 h. In other words, MgO nanoparticles have been successfully coated on the surface of nanocomposite by directly adding to A1 (MWCNT–COOH–cellulose–MgO; A2). In another reaction, MgO nanoparticles were added indirectly; for this, 0.5 g nanocomposite (A1) was ultrasonically dissolved in 1.5 ml Mg $(NO_3)_2$ (1 M) for 2 h, then the dispersion was centrifuged at 12,000 rpm for 10 min, the supernatant was removed, and 1.5 ml water was added. This washing step was repeated four times. Then reaction solution was filtered with deionized water. Eventually, we put it in the oven at 50 °C for 24 h, MgO nanoparticles were achieved by coating indirectly on the surfaces (MWCNT–COOH–cellulose–MgO; A3).

Adsorption study

Capacity of methylene blue removal from aqueous solution by A1, A2, and A3 adsorbents was determined by adding 20.0 mg of each of the adsorbents into 20.0 mL of methylene blue dye solution (10.0–50.0 mg/L); all samples were contacted at certain time periods, 5, 10, 15, 20, 25, 30, 35, 40, 45, 50, 55, 60 and 65 min, in the kinetic experiments at room temperature. After certain time, to determine the amount of MB dye adsorption on nanocomposite surfaces, the samples that contain methylene blue dye and nanocomposite were filtered by a 0.22-μm membrane filter and MB dye suspensions containing A1, A2, and A3 adsorbents were centrifuged at 4000 rpm for 5 min using a centrifuge (5702R Pendorf, Germany). The remaining methylene blue concentrations were analyzed using a UV–Vis spectrophotometer furnished by Varian (Cary 100 Bio) (London, England) at maximum wavelength of 668 nm. To determine MB adsorption capacity onto A1, A2, and A3 as nanocomposite adsorbents at time t (q_t), in mg/g, the following equation was used [20]:

$$q_t = \left(\frac{C_0 - C_t}{W}\right) \times V, \tag{1}$$

where q_t is the methylene blue (Fig. 1) dye adsorption capacity at time t (mg/g), C_0 is the MB initial concentration (mg L^{-1}), C_t is the MB dye concentration at time t (mg L^{-1}), V is the methylene blue dye solution volume (L) and W is the mass of nanocomposite adsorbents (g). To evaluate the isotherm and kinetic fitness equations to the adsorption experimental data we used the average relative error (ARE) that can be presented as [21]:

$$\text{ARE}\ (\%) = \frac{100}{n} \sum_{i}^{n} \left| \frac{q_{i,cal} - q_{i,\exp}}{q_{i,\exp}} \right|, \tag{2}$$

where N is the data point number. To confirm the results, each experiment was conducted in triplicate under the same conditions and was found reproducible.

Results and discussion

Characterization

The FT-IR spectrophotometer (Perkin–Elmer Spectrum 100, USA) was used to detect changes in chemical bonding and structure in the frequency range of 4000–480 cm^{-1}. FT-IR spectra of A1, A2, and A3 are presented in Fig. 2. After oxidation, the presence of carboxylic groups was confirmed by C=O stretching band that appeared at approximately 1737 cm^{-1}, whereas the absorption band at 600–900 cm^{-1} and several low-intensity peaks were attributed to C–O stretching vibrations of the –COOH groups. The relatively increased band intensities between 3400 and 3600 cm^{-1} suggest more –OH groups on the surface of the MWCNTs after oxidation and water treatment (Fig. 2). Morphology of all adsorbents (A_1, A_2, and A_3 surface adsorbents) was investigated by TEM and observed as black line regions in MWCNT–COOH (Fig. 3).

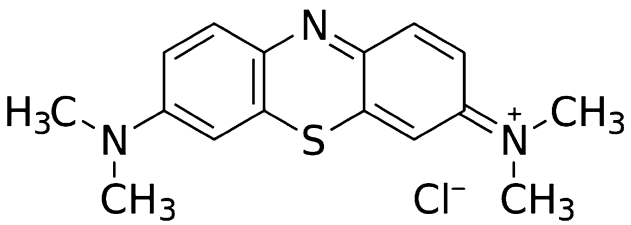

Fig. 1 Structure of methylene blue dye

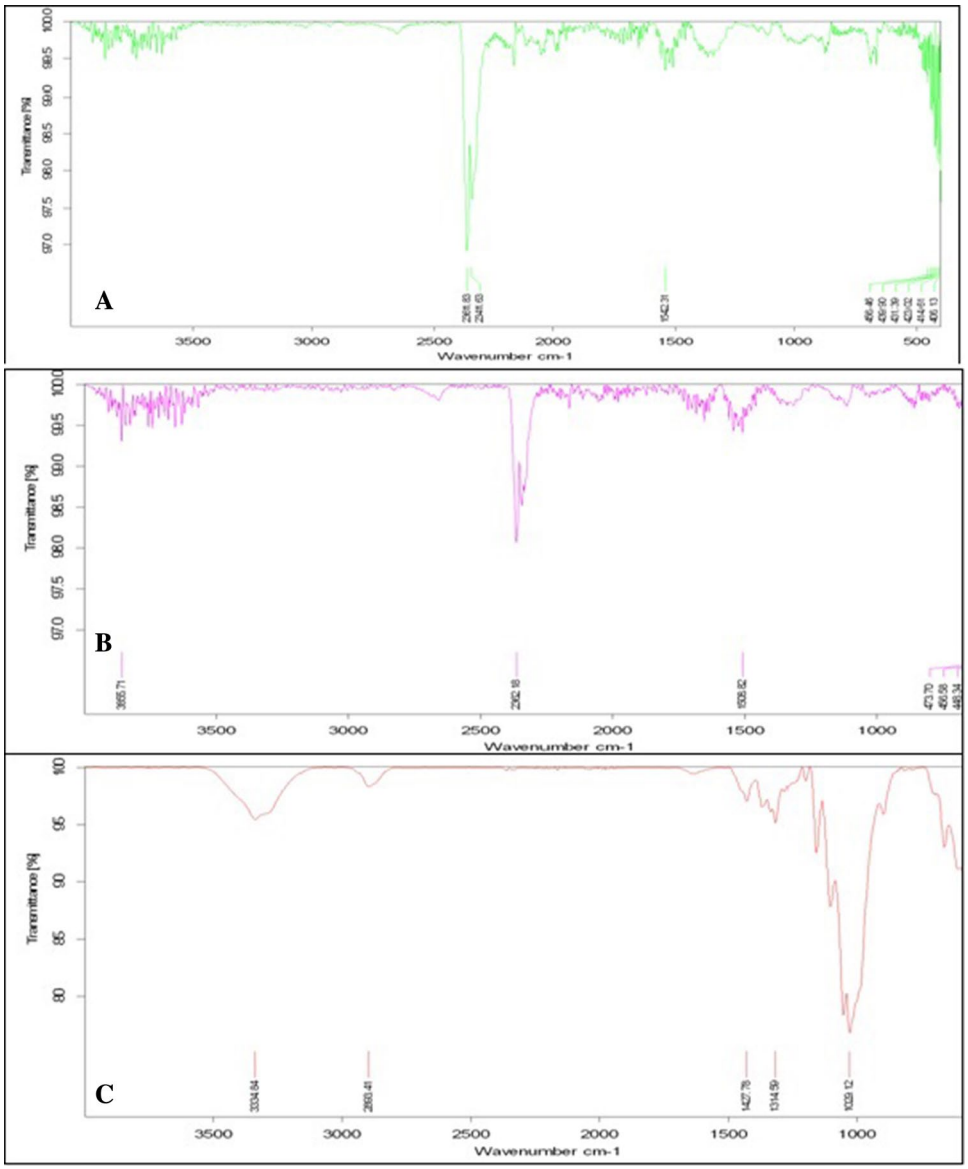

Fig. 2 FTIR image of **a** A1 MWCNT–COOH–cellulose adsorbent, **b** A2 adsorbent with MgO directly, and **c** A3 adsorbent with MgO nanoparticles indirectly

Scanning electron microscope (SEM) images of nanocomposite surfaces are presented in Fig. 4. The morphology of the prepared fibers was examined by scanning electron microscope (SEM, Ultra 55, Carl Zeiss SMT AG, Germany). The samples for SEM investigations were coated with a 5-nm-thick platinum layer. Characterization of dispersion state of A1 in cellulose and fractured surfaces of nanocomposite films was examined by SEM. Pure cellulose has homogeneous and smooth surface. In contrast, MWCNT–COOH has rougher surfaces and lots of humps, perhaps caused by the wrinkles of MWCNT–COOH sheets, and this results in a larger number of potential adsorption sites. A1 adsorbent is well dispersed in cellulose, as shown in Fig. 4a. In addition, dispersion of MgO nanoparticles by direct and indirect method in A1 adsorbent was observed, as shown in Fig. 4b, c. High-vacuum conditions were applied and high efficiency In-lens SE detector was used for image acquisition. X-ray diffraction (XRD) patterns of A1 adsorbent and with MgO nanoparticles by direct method (A2), and with MgO nanoparticles by indirect method (A3) are shown in Fig. 5. XRD pattern of A1 adsorbent revealed two peaks at 25.7° and 43.6°, which correspond to interlayer spacing (0.34 nm) of MWCNTs (d002) and the d100 reflection of the MWCNT–COOH, respectively. Peaks at $2\theta = 41.1°$, 42.9°, 62.2°, and 78.7° correspond to MgO nanoparticle. Moreover, the mean crystallite size of the nanocrystalline MgO nanoparticle material was estimated using the Scherrer formula and found to be in the range of 20–38 nm (Fig. 5).

Effect of contact time

Effect of contact time on methylene blue dye adsorption process was investigated. All nanocomposite, MWCNT–COOH–cellulose (A1), MWCNT–COOH

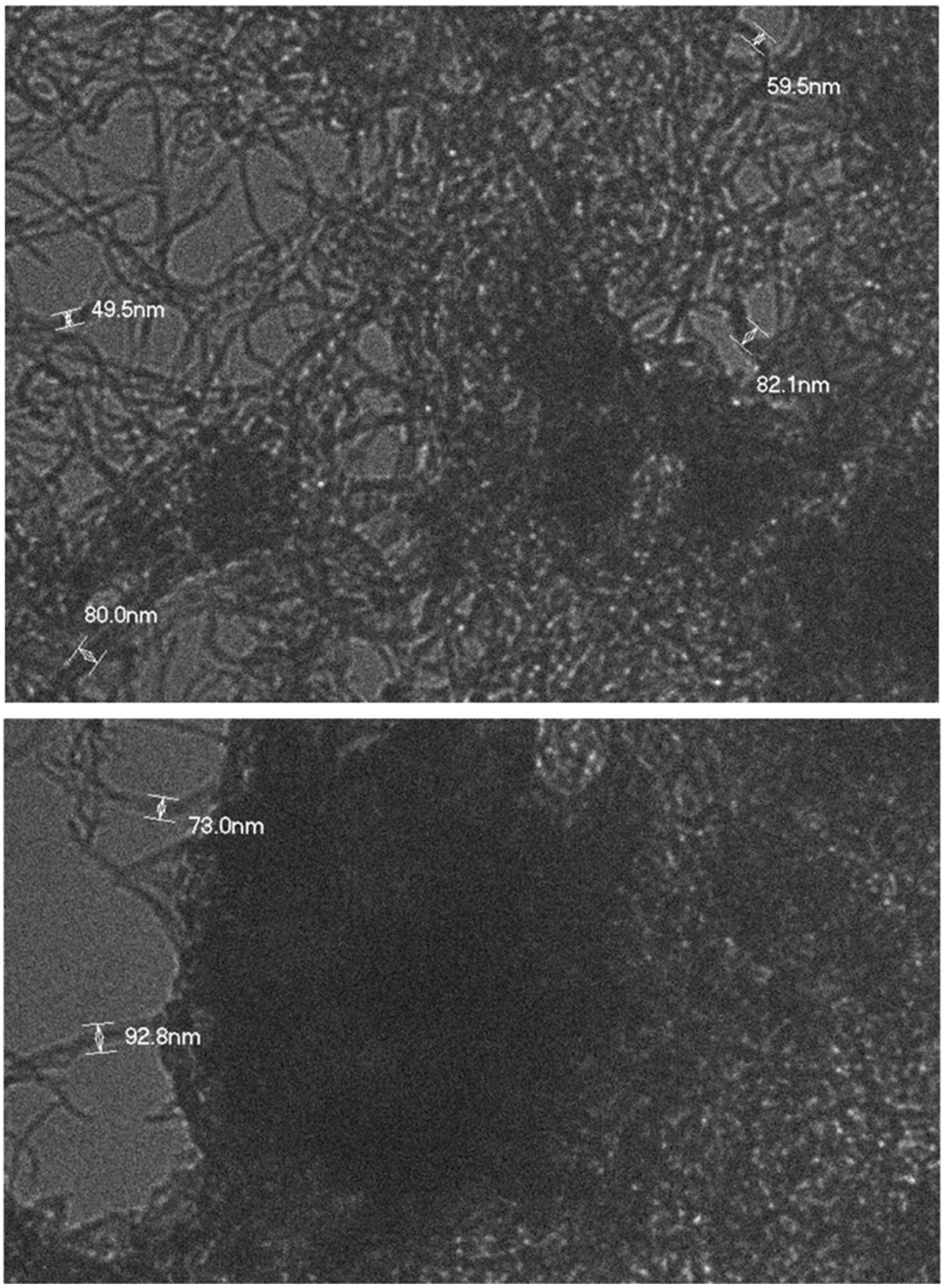

Fig. 3 TEM image of **a** A1MWCNT–COOH–cellulose adsorbent, **b** A2 adsorbent with MgO directly, and **c** A3 adsorbent with MgO nanoparticles indirectly

–cellulose with MgO directly (A2), and MWCNT–COOH–cellulose with MgO indirectly(A3), surfaces as adsorbents contacted with methylene blue dye in aqueous solutions with 0.3 mg/lit concentration at $T = 298$ K. For analyzing the concentration of methylene blue dye in solution before and after adsorption processes, the UV–Vis spectrophotometer was used. The curve of methylene blue dye amount adsorbed on the MWCNT–COOH–cellulose (A1), MWCNT–COOH–cellulose with MgO directly (A2), and MWCNT–COOH–cellulose with MgO indirectly (A3) surfaces as adsorbent is shown in Fig. 6 as a function of contact time. According to the results, 55 min was selected as the best contact time between methylene blue dye and all three nanocomposites.

Effect of initial dye concentration

Initial dye concentration is widely effective on dye removal. Effect of initial dye concentration relies on the immediate relation between the active binding sites on the adsorbent

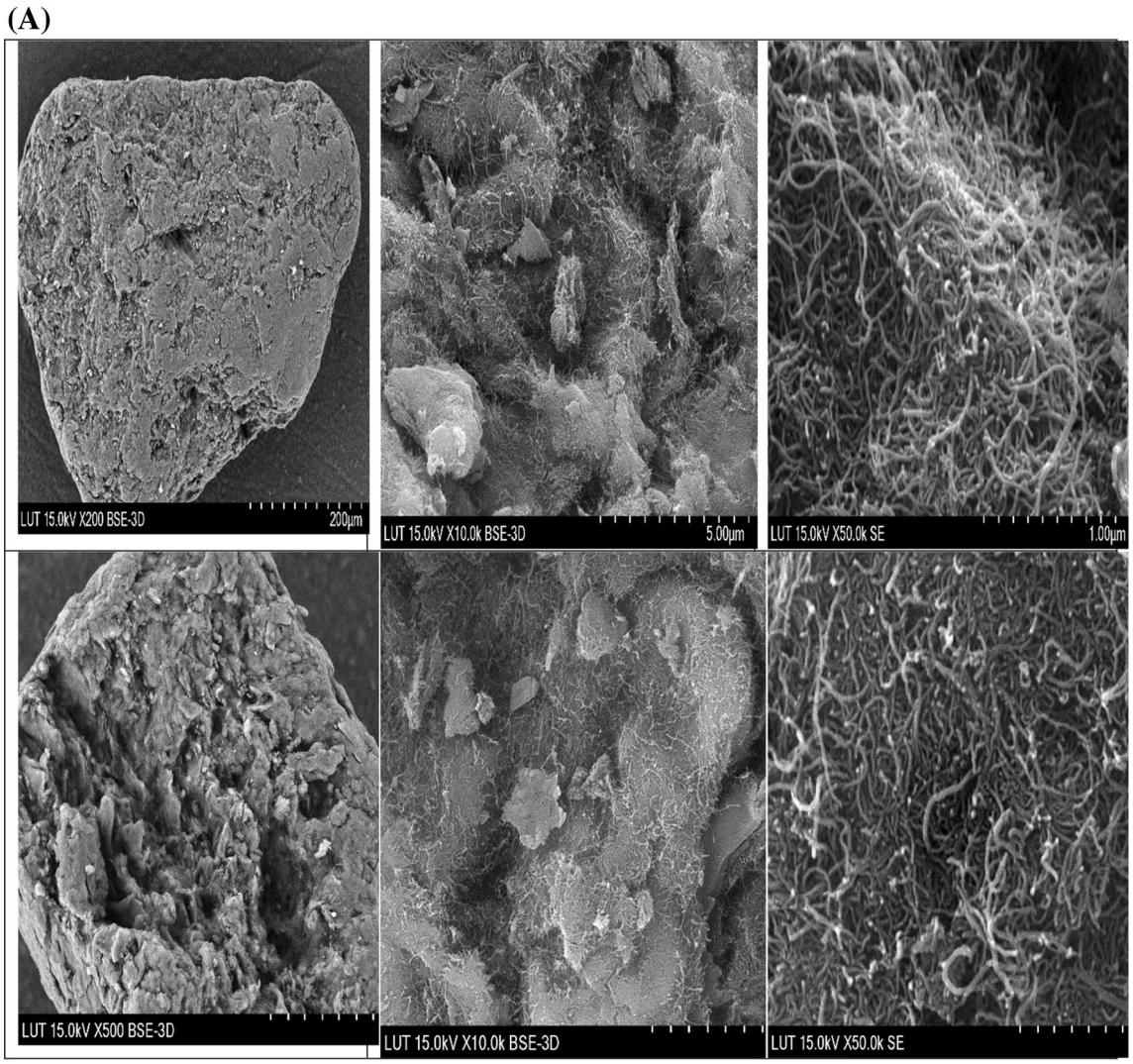

Fig. 4 SEM image of **a** MWCNT–COOH–cellulose A1 adsorbent, **b** A1 adsorbent with MgO directly, and **c** A1 adsorbent with MgO indirectly. These images are taken in three different zones

surface and dye concentration. An increase in the initial concentration of dye will improve the efficiency of dye removal according to the increased interaction of dye and absorbent surface [21–23]. In this study, the effect of initial concentration of dye on adsorption capacity of methylene blue dye onto MWCNT–COOH–cellulose (A1), MWCNT–COOH–cellulose with MgO directly (A2), and MWCNT–COOH–cellulose with MgO indirectly (A3) surfaces as adsorbents was investigated. As shown in Fig. 7, by increasing the initial concentration of methylene blue dye the adsorption capacity will increase; this may increase the interaction and collisions between dye molecules and adsorbent surfaces.

Effect of temperature

Temperature is one of the main factors in the adsorption process. For several dyes and absorbents, adsorption process can be endothermic or exothermic in nature. If dye removal efficiency increases with increasing the solution temperature it can be concluded that the dye adsorption process on adsorbent surface is endothermic; on the other hand, if with increasing the solution temperature the efficiency of dye removal decreases, dye adsorption process will be exothermic in nature [22, 23]. The relationship between the temperature and the removal of methylene blue dye by MWCNT–COOH–cellulose (A1), MWCNT–COOH–cellulose with MgO directly (A2), and MWCNT–COOH–cellulose with MgO indirectly (A3) as nanocomposite adsorbents was investigated

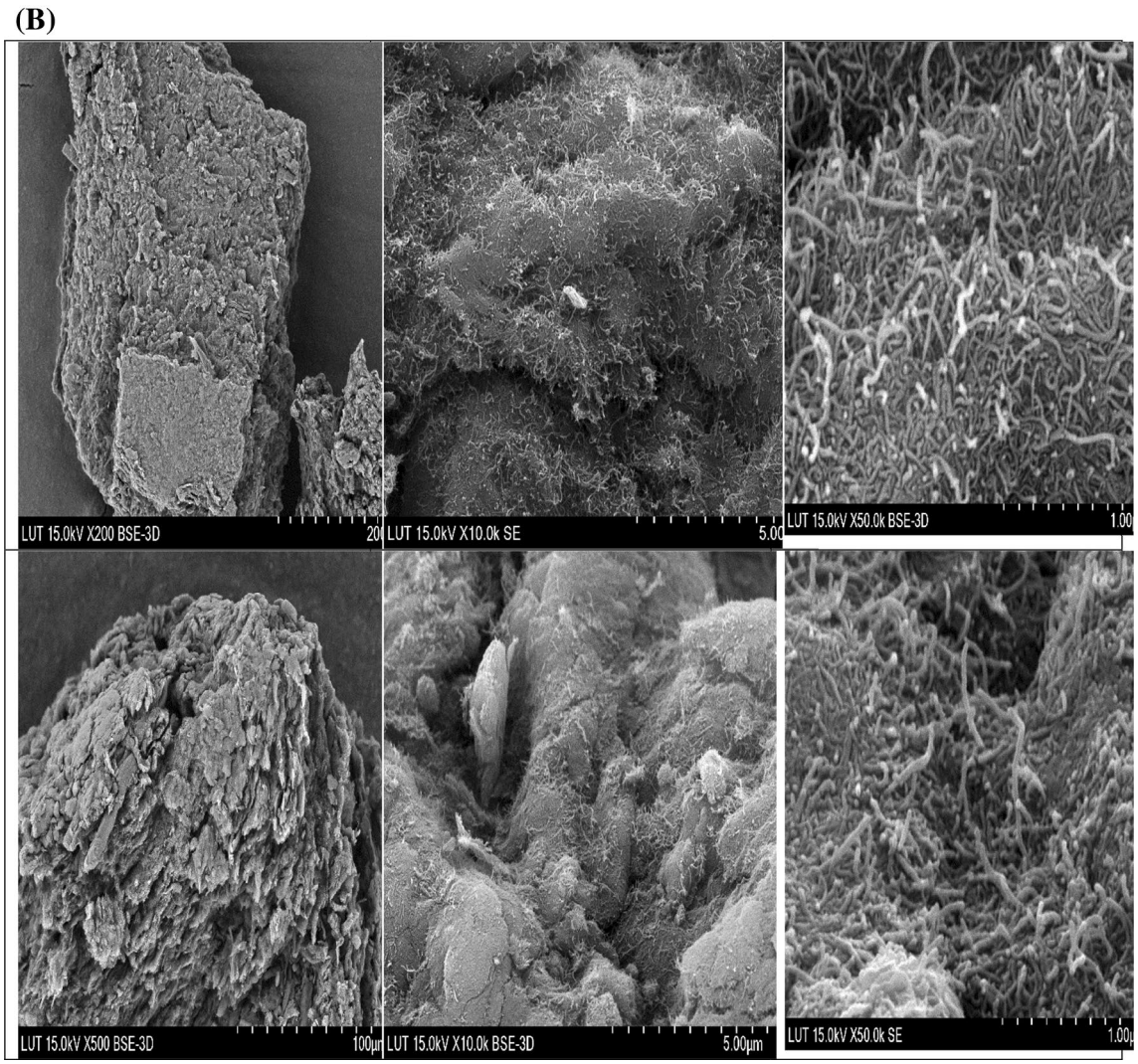

Fig. 4 (continued)

at different temperatures from 288 K to 308 K, respectively. We observed that with increasing the solution temperature, methylene blue dye removal efficiency by all three nanocomposite adsorbents was increased (Fig. 8). According to these results, adsorption of MB dye by MWCNT–COOH–cellulose (A1), MWCNT–COOH–cellulose with MgO directly (A2), and MWCNT–COOH–cellulose with MgO indirectly (A3) surfaces as adsorbents may be an exothermic process.

Adsorption thermodynamic

Temperature is the important parameter influencing the adsorbent capacity in adsorption process. According to the results of "Effects of temperature", the methylene blue dye adsorption capacity of all three adsorbents increases with increase in the temperature of solutions. It means that the adsorption of methylene blue dye onto nanocomposite surfaces is an exothermic process. Entropy (ΔS°), the adsorption free energy (ΔG°), and standard enthalpy (ΔH°) for methylene blue dye adsorption onto MWCNT–COOH–cellulose (A1), MWCNT–COOH–cellulose with MgO directly (A2), and MWCNT–COOH–cellulose with MgO indirectly (A3) surfaces were calculated to evaluate the MB dye removal thermodynamic feasibility using the adsorbents in this study [22–26]:

$$\Delta G^{\circ} = -RT \ln (55.5b), \tag{3}$$

$$\ln (55.5b) = \frac{\Delta S^{\circ}}{R} - \frac{\Delta H^{\circ}}{RT}, \tag{4}$$

$$\Delta G^{\circ} = \Delta H^{\circ} - T\,\Delta S^{\circ}, \tag{5}$$

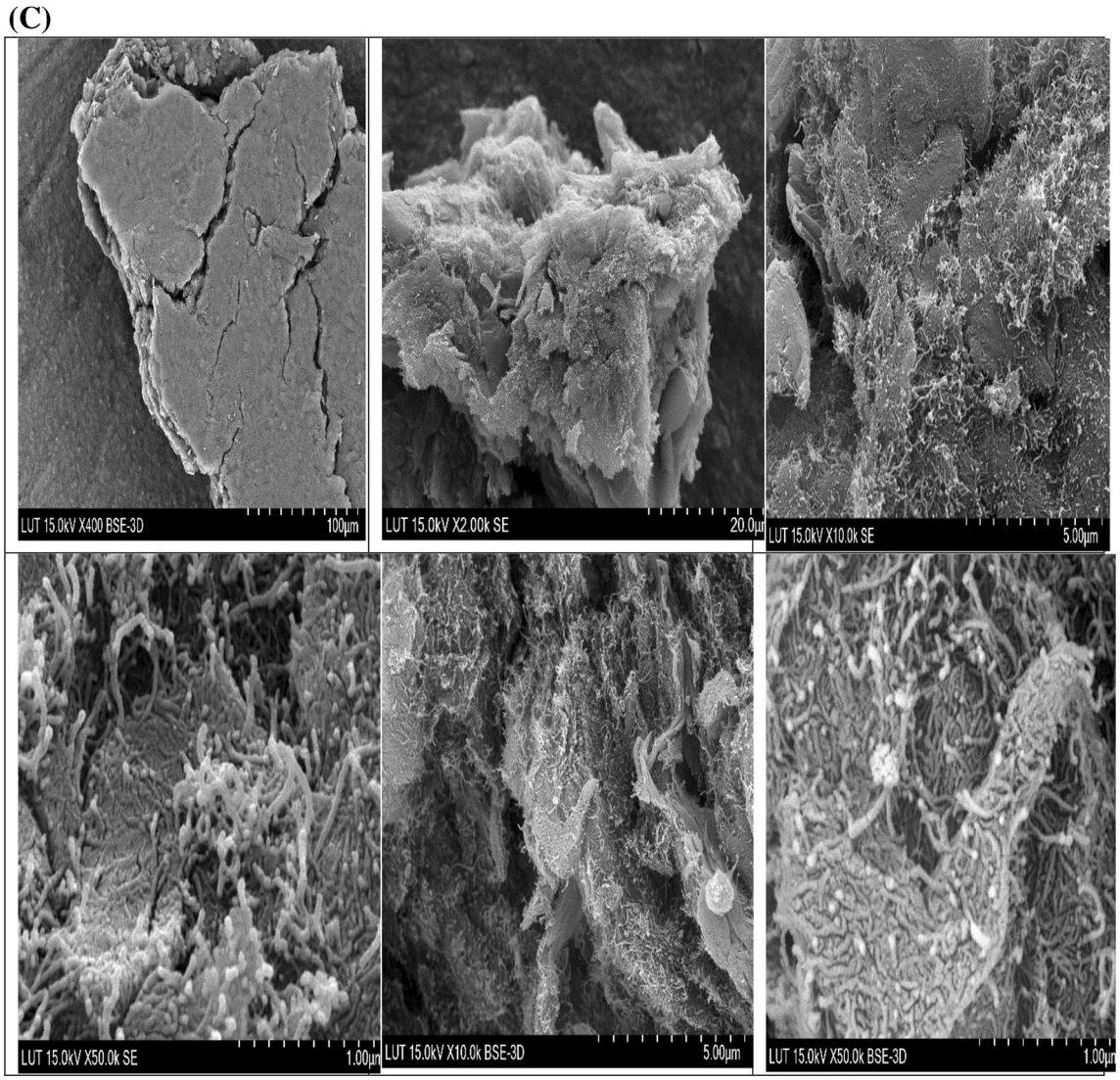

Fig. 4 (continued)

where T is the solution temperature (K) and R is the universal gas constant (8.314 J mol^{-1} K^{-1}). *b*, the Langmuir constant (type I) for adsorption process, was derived from the isotherm study. From the slope and intercept of the linear plots of ln (55.5*b*) versus 1/*T* (Fig. 9), ΔS° and ΔH° can be obtained, respectively. Best fit of data was confirmed by the low values of average relative error (ARE) and high values of R^2 of the estimated thermodynamic parameters (Table 1). Useful mechanism information of the adsorption process was demonstrated by the thermodynamic parameter values.

Adsorption equilibrium

Adsorption isotherms allow appraising the ability to use the adsorption process as a unit action, comparing the adsorption maximum capacities of materials as adsorbent. Also, the models of isotherm with best fit to the adsorption experimental data provide useful information about the adsorption nature [27, 28]. Figure 8 shows the linear fits of four types of Langmuir isotherm model and Figs. 9, 10 and 11 show the Freundlich, Temkin, and Halsey adsorption isotherm models for experimental data. The isotherm parameter values, the adsorption maximum capacity (q_{max}), the average relative error (ARE) and the coefficient determination (R^2) are listed in Tables 1 and 2. Adsorption isotherms of methylene blue dye onto MWCNT–COOH–cellulose (A1), MWCNT–COOH–cellulose with MgO directly (A2), and MWCNT–COOH–cellulose with MgO indirectly (A3) surfaces as nanocomposite adsorbents were compared. All the isotherm models presented a capillary steep, and condensation steep which is consistent with the adsorption in solution, that is a common characteristic in the mesoporous materials.

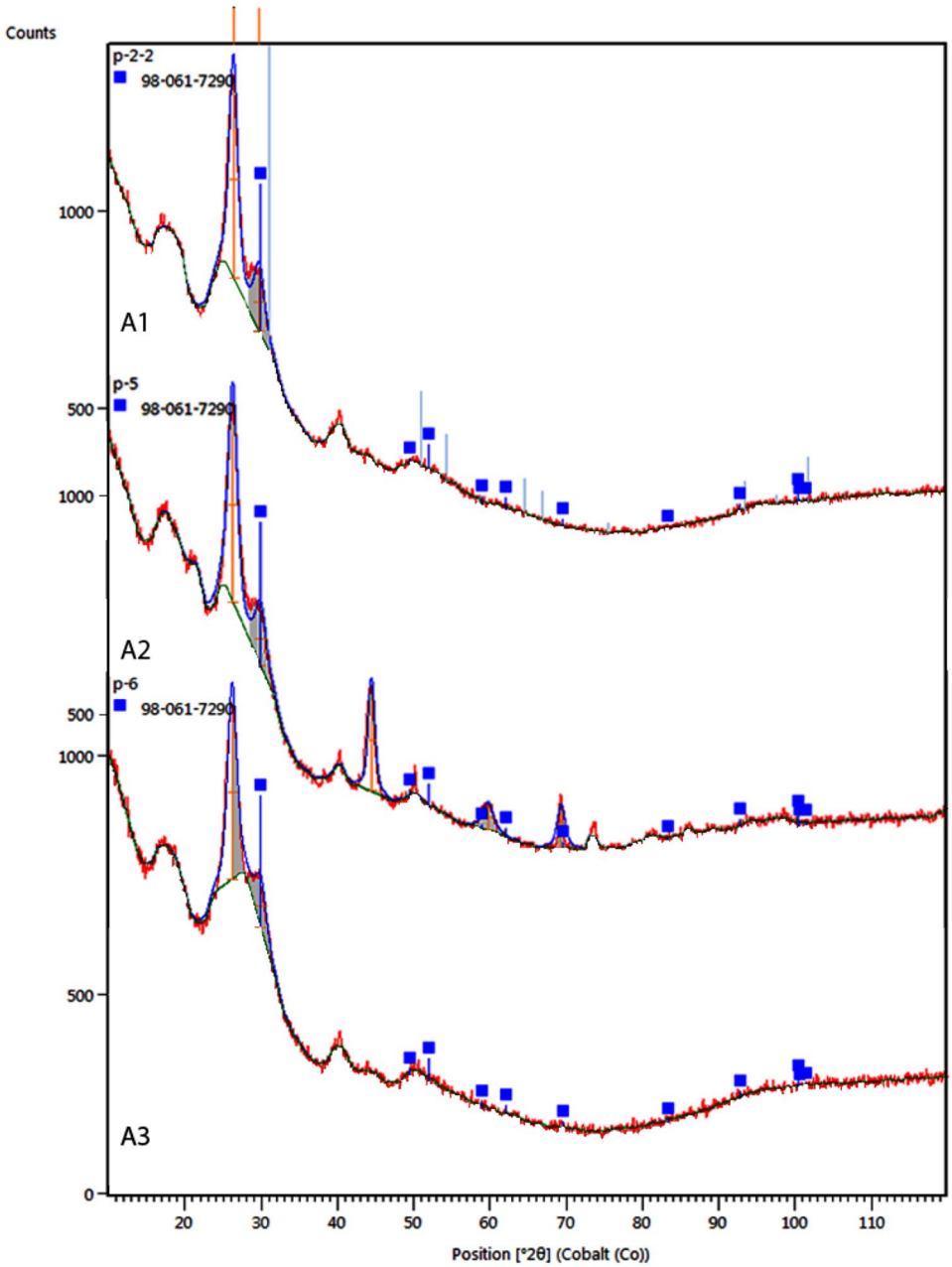

Fig. 5 X-ray powder diffraction of **a** MWCNT–COOH–cellulose A1 adsorbent, **b** A2 adsorbent with MgO directly, and **c** A3 adsorbent with MgO indirectly

Langmuir isotherm

There are four different types of linearized Langmuir isotherm models; we used a simple linear model in this study. The Langmuir isotherm model can be presented as:

$$q_e = \frac{Q_{\mathrm{mKC_e}}}{\left(1 + KC_{\mathrm{e}}\right)}, \tag{6}$$

where Q_{m} is the capacity of adsorption of methylene blue dye (mg/g) and K is the adsorption energy of methylene blue dye removal (L/mg) [29–32]. Four types of Langmuir isotherm models can be expressed as [33–35]:

$$\text{Type (I)} : \frac{Ce}{qe} = \frac{1}{KQm} + \frac{Ce}{Qm}, \tag{7}$$

$$\text{Type (II)} : \frac{1}{qe} = \frac{1}{Qm} + \frac{1}{KQmCe}, \tag{8}$$

$$\text{Type (III)} : q_{\mathrm{e}} = K - \frac{q_{\mathrm{e}}}{QmC_{\mathrm{e}}}, \tag{9}$$

$$\text{Type (IV)} : \frac{q_{\mathrm{e}}}{C_{\mathrm{e}}} = KQ_m - Kqe. \tag{10}$$

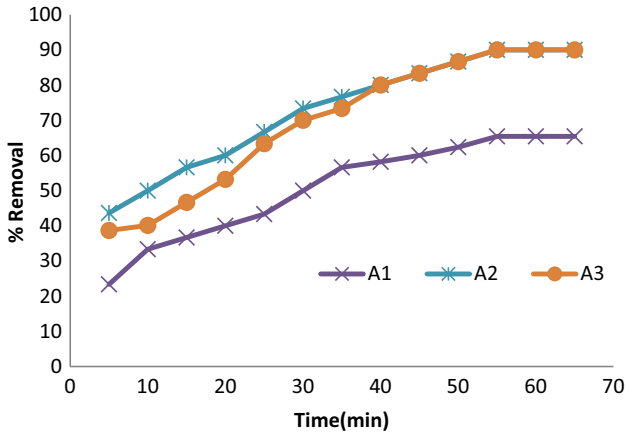

Fig. 6 Effect of contact time on the removal of MB dye with MWCNT–COOH–cellulose (A1), MWCNT–COOH–cellulose with MgO directly (A2), and MWCNT–COOH–cellulose with MgO indirectly (A3) surfaces as adsorbents. Conditions: time 5–65 min, C_0 0.3 mg/L of MB dye solution and temperature 298 K

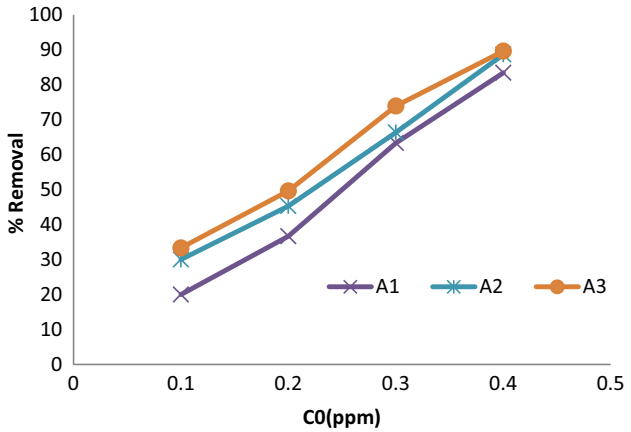

Fig. 7 Effect of initial concentration on the removal of MB dye with MWCNT–COOH–cellulose (A1), MWCNT–COOH–cellulose with MgO directly (A2), and MWCNT–COOH–cellulose with MgO indirectly (A3) surfaces as adsorbents. Conditions: time 55 min, C_0 0.1–0.5 mg/L of MB dye solution and temperature 298 K

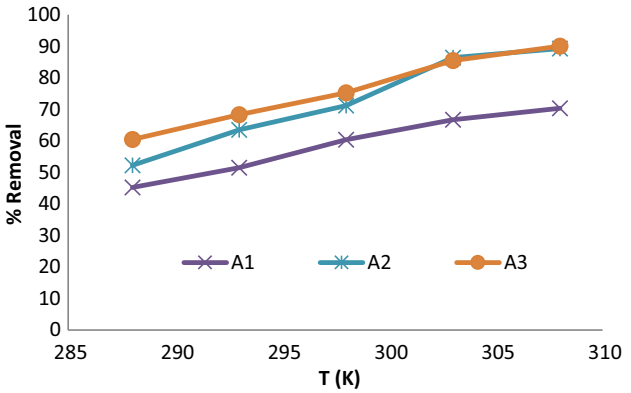

Fig. 8 Effect of temperature on removal of MB dye with MWCNT–COOH–cellulose (A1), MWCNT–COOH–cellulose with MgO directly (A2), and MWCNT–COOH–cellulose with MgO indirectly (A3) surfaces. Conditions: time 55 min and temperature 288–308 K

Freundlich isotherm

Isotherm study results show that Langmuir isotherm model gives the best fit over methylene blue dye concentration for MWCNT–COOH–cellulose (A1), MWCNT–COOH–cellulose with MgO directly (A2), and MWCNT–COOH–cellulose with MgO indirectly (A3) surfaces as nanocomposite adsorbents; however, it provides little insights into mechanism of physical adsorption. The values of constants are varying markedly with MB dye concentration. It can be presented by the following equation [36, 37]:

$$q_e = K_F C_e^{1/n}, \tag{11}$$

where K_F and $1/n$ are the Freundlich isotherm model constants [36, 37]. The Freundlich isotherm constants K_F and 1/n could be calculated from the plot of $\ln q_e$ versus $\ln C_e$ that is shown in Fig. 11.

Temkin isotherm

The indirect adsorption effects of interaction and substance adsorption on isotherms of adsorption are described by Temkin isotherm model (Fig. 12). Temkin isotherm

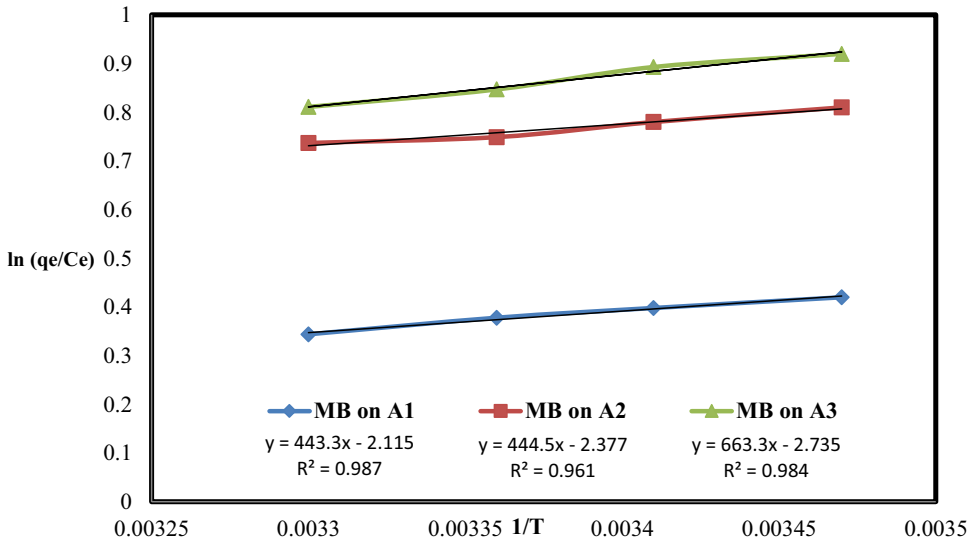

Fig. 9 The thermodynamic study (Van't Hoff plot) for the removal of MB dye with MWCNT–COOH–cellulose (A1), MWCNT–COOH–cellulose with MgO directly (A2), and MWCNT–COOH–cellulose with MgO indirectly (A3). Conditions: time 55 min and temperature 288–308 K

model describes the adsorption system behavior on a heterogeneous surface, which can be presented by the following equation [38, 39]:

$$q_e = B\ln(AC_e), \tag{12}$$

where A is the binding equilibrium constant corresponding to binding maximum energy and B is adsorption constant related to heat and is equal to RT/b [39], as shown in Fig. 10. The plot of qe versus $\ln C_e$ is used to define constants of isotherm of Temkin.

Table 1 Thermodynamic of parameters for the removal of MB dye with MWCNT–COOH–cellulose (A1), MWCNT–COOH–cellulose with MgO directly (A2), and MWCNT–COOH–cellulose with MgO indirectly (A3) surfaces. Conditions: time 55 min and temperature 288–308 K

Adsorbent	T (K)	Functions		
		ΔS°(kJ/mol K)	ΔH°(kJ/mol)	°GΔ (kJ/mol)
A1	288	0.0176	− 3.686	− 1.383
	293			− 1.471
	298			− 1.559
	303			− 1.647
A2	288	0.0198	− 3.696	− 2.006
	293			− 2.105
	298			− 2.204
	303			− 2.303
A3	288	0.0227	− 5.515	− 1.023
	293			− 1.136
	298			− 1.249
	303			− 1.363

The Halsey isotherm

The equation of Halsey isotherm model can be presented by [35–38]:

$$\ln q_e = \left[\left(\frac{1}{n}\right)\ln K - \left(\frac{1}{n}\right)\ln C_e\right]. \tag{13}$$

The multi-layer adsorption is explained by Halsey equation very well; if the Halsey isotherm well fits the equilibrium data, the adsorbent is heterogeneous in nature. The plot of $\ln q_e$ versus $\ln C_e$ for the removal of MB dye with MWCNT–COOH–cellulose (A1), MWCNT–COOH–cellulose with MgO directly (A2), and MWCNT–COOH–cellulose with MgO indirectly (A3) surfaces is shown in Fig. 13.

Adsorption kinetic study

Adsorption kinetic study was conducted to investigate the effects of contact time and achieve the resulting parameters of adsorption process. Figure 4 shows the contact time and the methylene blue dye adsorption capacity change of MWCNT–COOH–cellulose (A1), MWCNT–COOH–cellulose with MgO directly (A2), and MWCNT–COOH–cellulose with MgO indirectly (A3) surfaces as a function of time. There was no obvious change in the MB absorption capacity of nanocomposite adsorbent surface after 55 min. Therefore, 55 min was selected as the best contact time for all the methylene blue dye adsorption experiments onto the MWCNT–COOH–cellulose (A1),MWCNT–COOH–cellulose with MgO directly (A2), and MWCNT–COOH–cellulose with MgO indirectly (A3) surfaces. The methylene blue adsorption process kinetics

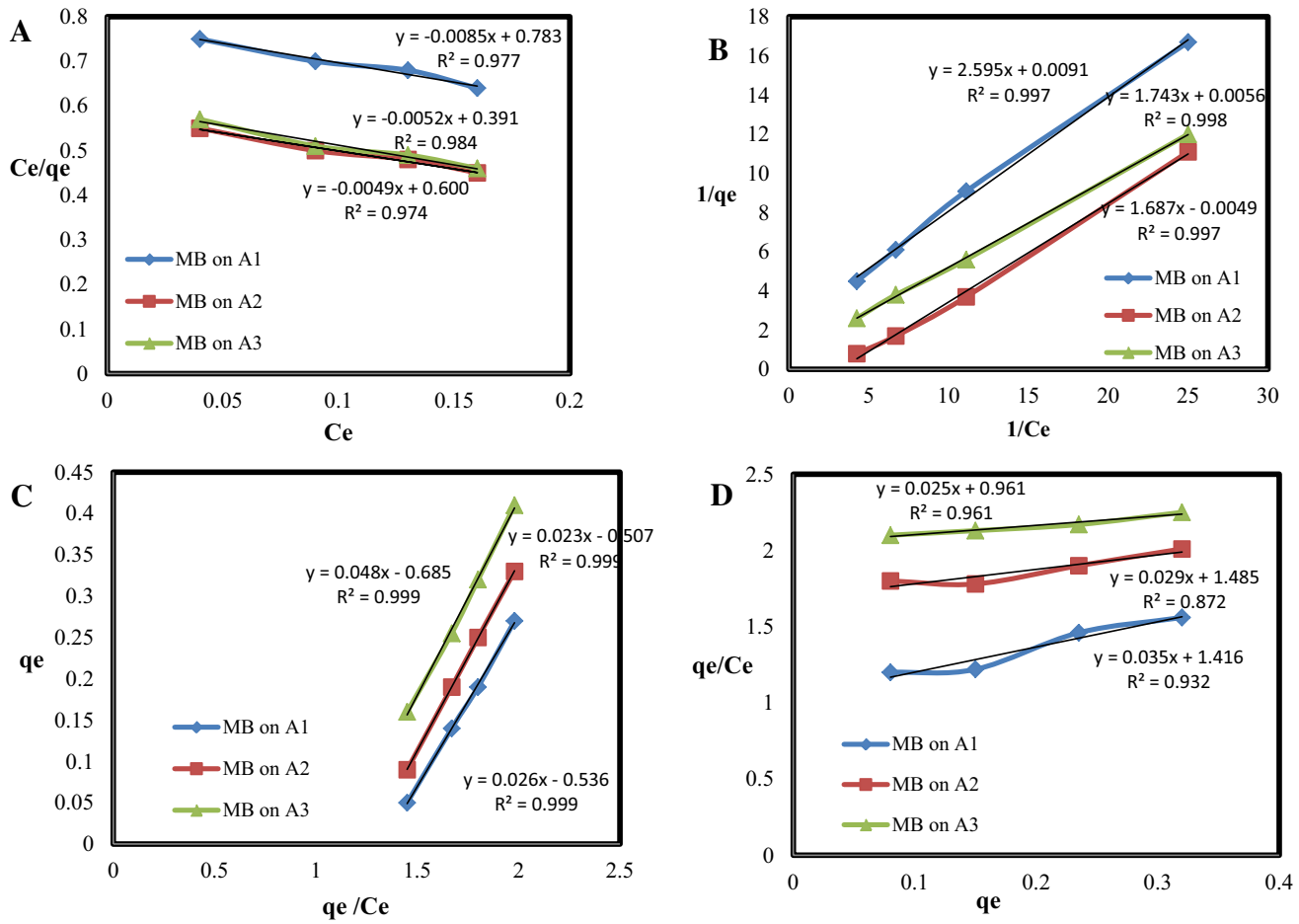

Fig. 10 Langmuir isotherms for the removal of MB dye with MWCNT–COOH–cellulose (A1), MWCNT–COOH–cellulose–MgO (A2), and MWCNT–COOH–cellulose–MgO NPs (A3) surfaces. **a** Type 1, **b** Type 2, **c** Type 3, and **d** Type 4. MWCNT–COOH–cellulose (A1), MWCNT–COOH–cellulose with MgO directly (A2), and MWCNT–COOH–cellulose with MgO indirectly (A3). Conditions: time 55 min, C_0 0.1–0.5 mg/L of MB dye solution and temperature 298 K

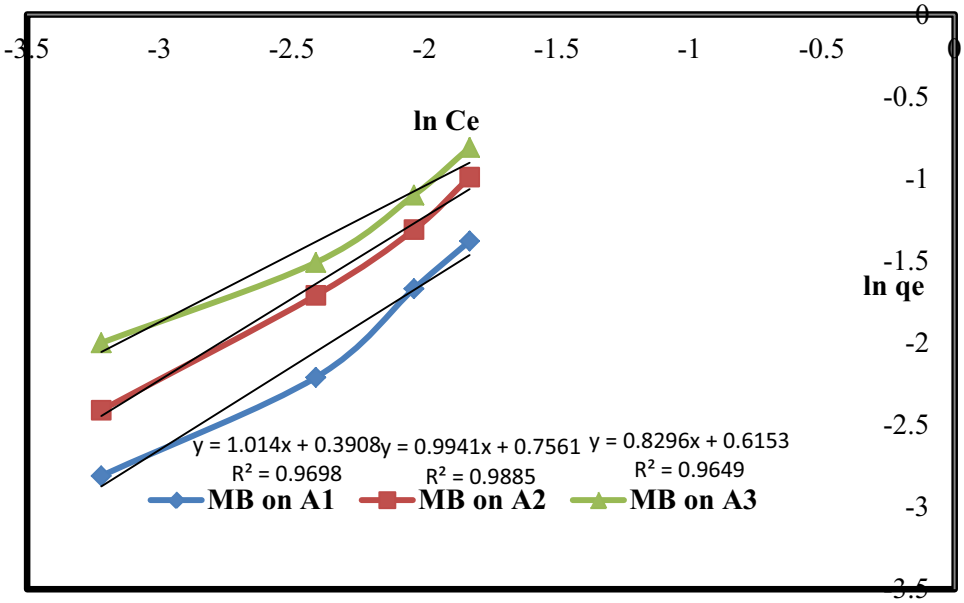

Fig. 11 Freundlich isotherms for the removal of MB dye with MWCNT–COOH–cellulose (A1), MWCNT–COOH–cellulose with MgO directly (A2), and MWCNT–COOH–cellulose with MgO indirectly (A3) surfaces. Conditions: time 55 min, C_0 0.1–0.5 mg/L of MB dye solution and temperature 298 K

Table 2 Langmuir isotherm parameters and ARE parameter for the removal of MB dye with MWCNT–COOH–cellulose (A1), MWCNT–COOH–cellulose with MgO directly (A2), and MWCNT–COOH–cellulose with MgO indirectly (A3) surfaces

Isotherm	Type	Equation	Dye		MG	
			Adsorbent	A1	A2	A3
Langmuir			*Qm*	172.41	192.31	204.08
	Type 1	$\frac{Ce}{qe} = \frac{1}{KQm} + \frac{Ce}{Qm}$	K(L/mg)	3.676	4.462	0.013
			R^2	0.977	0.984	0.974
			ARE (%)	3.48	3.62	3.11
			Qm	109.89	178.57	208.33
	Type 2	$\frac{1}{qe} = \frac{Ce}{Qm} + \frac{1}{KQmCe}$	*K* (L/mg)	0.004	0.004	0.003
			R^2	0.997	0.998	0.997
			ARE (%)	1.41	1.78	2.09
			Qm	71.42	43.47	38.46
	Type 3	$q_e = K - \frac{qe}{QmCe}$	*K* (L/mg)	0.308	0.507	0.207
			R^2	0.999	0.999	0.999
			ARE (%)	1.39	1.48	1.50
			Qm	38.44	34.48	40.45
	Type 4	$\frac{qe}{Ce} = kQ_m - kq_e$	*K* (L/mg)	0.025	0.029	0.035
			R^2	0.932	0.872	0.961
			ARE (%)	3.24	4.39	3.30

(A) Type 1, (B) Type 2, (C) Type 3, and (D) Type 4. Conditions: time 55 min, C_0 0.1–0.5 mg/L of MB dye solution and temperature 298 K

was studied by applying the pseudo-first-order, four types of the pseudo-second-order, the Elovich, and the intra-particle diffusion kinetic models (Table 3).

The pseudo-first-order model

Generally, in the studies of kinetic adsorption, the equation of pseudo-first-order model is presented as follows [39, 40]:

$$\frac{dq_t}{d_t} = k_1(qe - qt). \tag{14}$$

Integrated form of the pseudo-first-order equation is [40]:

$$\log\left(q_e - q_t\right) = \log q_e - \left(k_1/2.303\right)t. \tag{15}$$

In this study, q_e and q_t are the amount of methylene blue adsorbed on MWCNT–COOH–cellulose

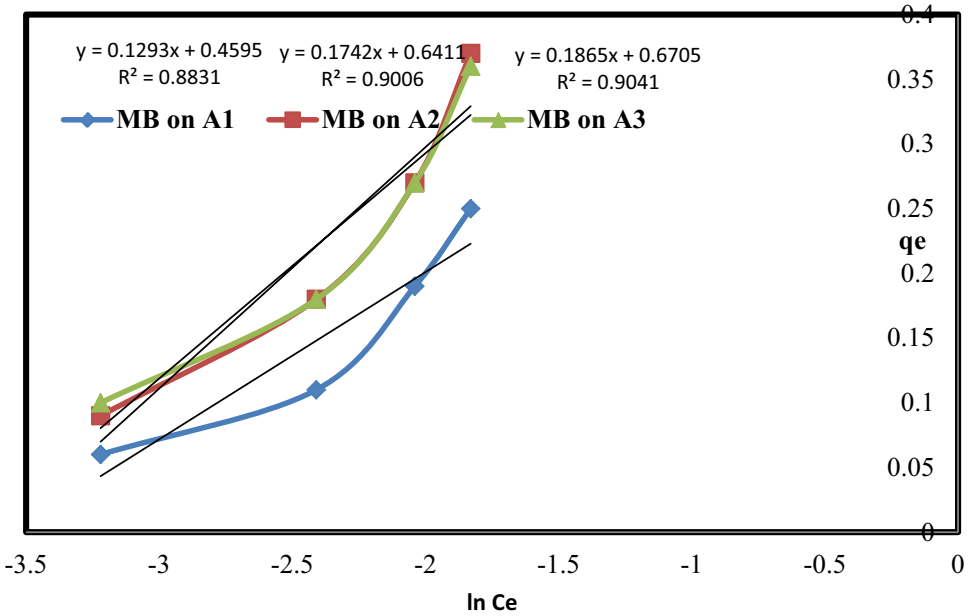

Fig. 12 Temkin isotherms for the removal of MB dye with MWCNT–COOH–cellulose (A1), MWCNT–COOH–cellulose with MgO directly (A2), and MWCNT–COOH–cellulose with MgO indirectly (A3) surfaces. Conditions: time 55 min, C_0 0.1–0.5 mg/L of MB dye solution and temperature 298 K

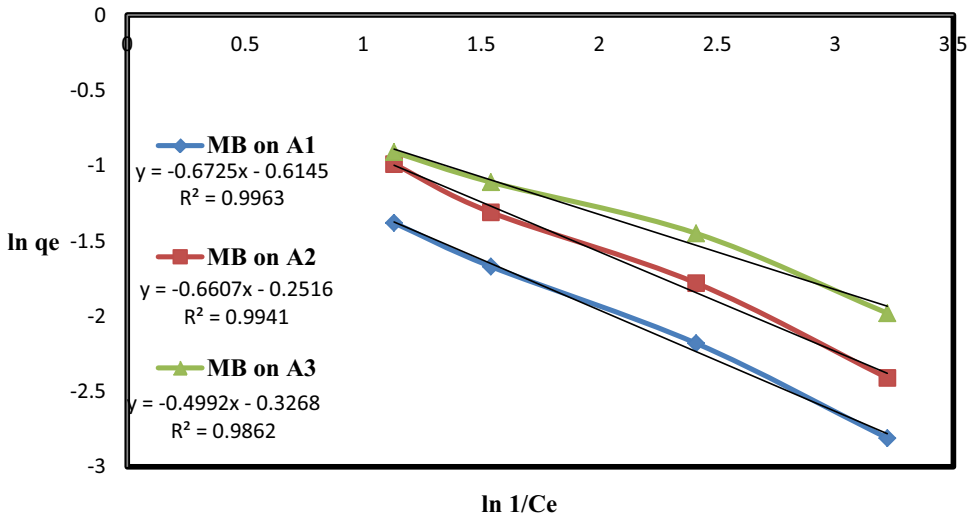

Fig. 13 Halsey isotherm for the removal of MB dye with MWCNT–COOH–cellulose (A1), MWCNT–COOH–cellulose–MgO (A2), and MWCNT–COOH–cellulose–MgO NPS (A3) surfaces. Conditions: time 55 min, C_0 0.1–0.5 mg/L of MB dye solution and temperature 298 K

Table 3 The Freundlich, Temkin and Halsey isotherm parameters for the removal of MB dye with MWCNT–COOH–cellulose (A1),MWCNT–COOH–cellulose with MgO directly (A2), and MWCNT–COOH–cellulose with MgO indirectly (A3) surfaces. Conditions: time 55 min, C_0 0.1–0.5 mg/L of MB dye solution and temperature 298 K

Isotherm	Equation	Parameters	Dye	MB		
			Adsorbent	A1	A2	A3
Freundlich	$\ln q_e = lnK_F + \frac{1}{n} lnCe$	K_F		1.477	2.130	1.850
		$1/n$		1.014	0.994	0.829
		R^2		0.969	0.988	0.964
		ARE (%)		5.31	5.98	4.34
Temkin	$q_e = B \ln(k_{Te} C_e))$	B (J/mol)		0.129	0.174	0.186
		K_{Te}		35.098	39.802	36.677
		R^2		0.883	0.900	0.904
		ARE (%)		6.84	5.29	5.27
Halsey	$\ln_{qe} = \left[\left(\frac{1}{n}\right) \ln K\right] - \left(\frac{1}{n}\right) \ln C_e$	K_{He}		1.511	1.180	1.177
		n		0.672	0.660	0.499
		R^2		0.996	0.994	0.986
		ARE (%)		3.85	3.21	4.08

(A1),MWCNT–COOH–cellulose with MgO directly (A2), and MWCNT–COOH–cellulose with MgO indirectly (A3) surfaces at equilibrium and at time t, respectively. K_1 is the rate constant of the pseudo-first-order model. According to Eq. (15), k_1 and q_e for MB adsorption on nanocomposite adsorbents can be determined by the slope and intercept plot of log ($q_e - q_t$) versus t that is shown in Fig. 14.

The pseudo-second-order model

For the kinetic studies of adsorption, the pseudo-second-order model presented by Ho in 1995 is expressed as the following that illustrated how the pertained adsorption rate related to the amount of equilibrium [41, 42]:

$$\frac{dq_t}{dt} = k\left(q_e - q_t\right)^2. \tag{16}$$

Linear form of pseudo-second-order model is presented as [41, 42]

$$\frac{t}{q_t} = \frac{1}{k_2 qe^2} + \frac{t}{q}, \tag{17}$$

in this study, k_2 is the constant rate of the pseudo-second-order model equilibrium of methylene blue adsorption onto the MWCNT–COOH–cellulose (A1), MWCNT–COOH–cellulose with MgO directly (A2), and MWCNT–COOH–cellulose with MgO indirectly (A3) surfaces (g/mg.min), t is the MB dye adsorption reaction time (min); q_e is the amount of MB dye removed by methylene blue adsorption onto the MWCNT–COOH–cellulose (A1),MWCNT–COOH–cellulose with MgO directly (A2), and MWCNT–COOH–cellulose with MgO indirectly (A3) surfaces at equilibrium (mg g^{-1}), and $q_t$is the amount of MB dye removed by

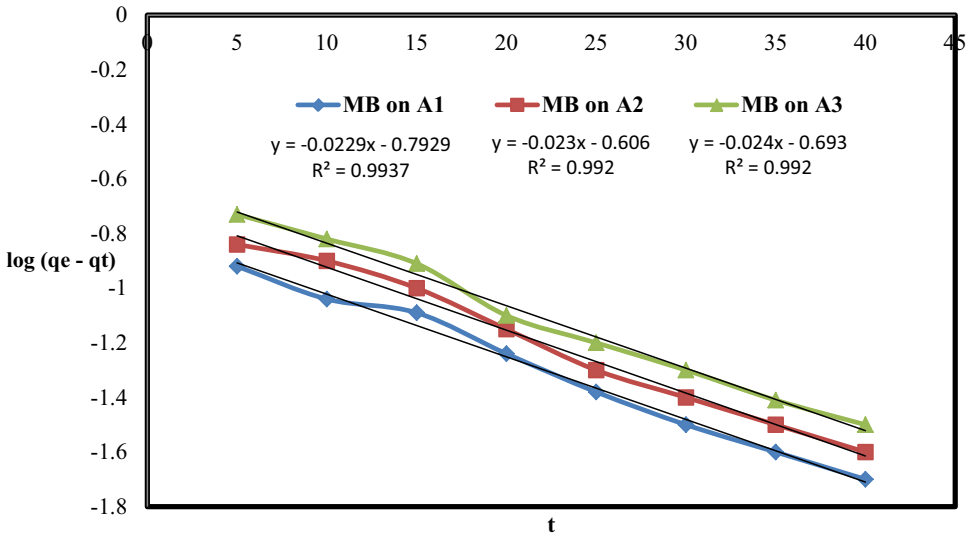

Fig. 14 The pseudo-first-order kinetic for the removal of MB dye with MWCNT–COOH–cellulose (A1), MWCNT–COOH–cellulose with MgO directly (A2), and MWCNT–COOH–cellulose with MgO indirectly (A3) surfaces

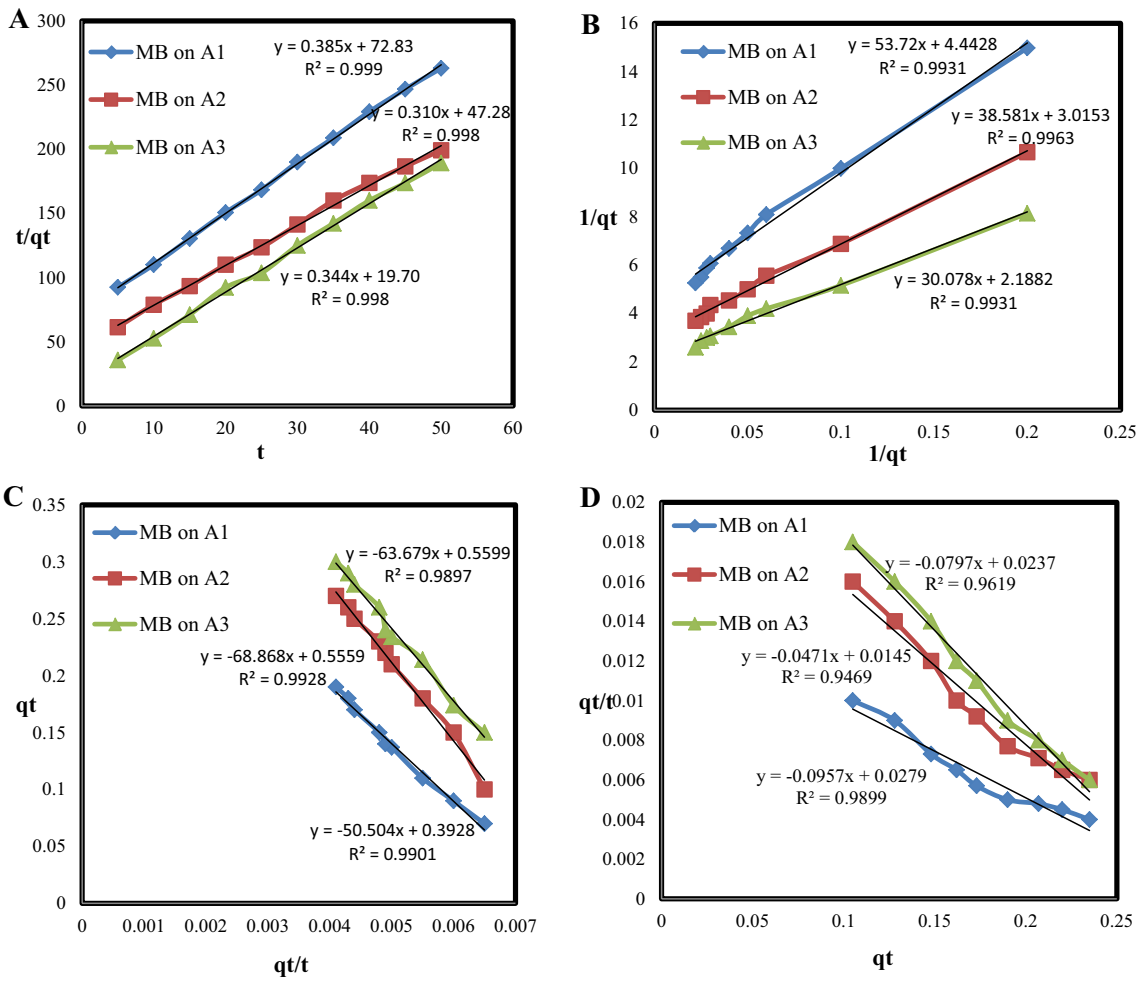

Fig. 15 The pseudo-second-order kinetic models for the removal of MB dye with MWCNT–COOH–cellulose (A1), MWCNT–COOH–cellulose with MgO directly (A2), and MWCNT–COOH–cellulose with MgO indirectly (A3) surfaces. (A) Type (I), (B) Type (II), (C) Type (III), and (D) Type (IV)

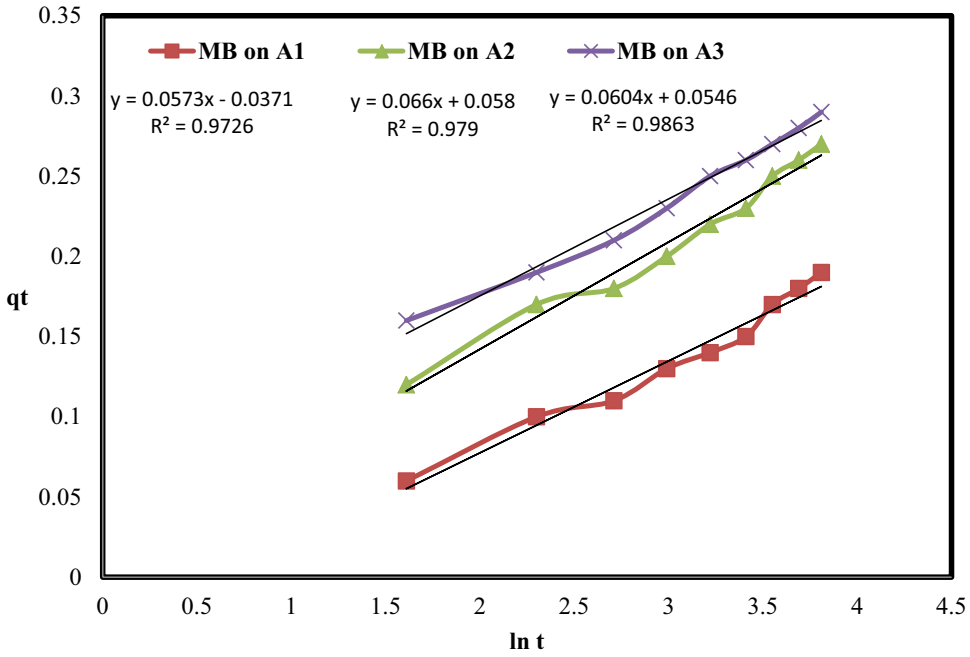

Fig. 16 The Elovich kinetic models for the removal of MB dye with MWCNT–COOH–cellulose (A1), MWCNT–COOH–cellulose with MgO directly (A2), and MWCNT–COOH–cellulose with MgO indirectly (A3) surfaces

nanocomposite surface at time t (mg g^{-1}). In this work, we used four types of linear form of the pseudo-second-order model. Here the plots of the pseudo-second-order model in different linear forms in types (I), (II), (III) and (IV) are shown in Fig. 15 [39, 40].

The Elovich model

Generally, the Elovich equation has been widely used in adsorption kinetics [41–43]:

$$\frac{d_{qt}}{dt} = \alpha \exp\left(-\beta q^2\right). \tag{18}$$

Table 4 Kinetic parameters of pseudo-second-order models for the removal of MB dye with MWCNT–COOH–cellulose (A1),MWCNT–COOH–cellulose with MgO directly (A2), and MWCNT–COOH–cellulose with MgO indirectly (A3) surfaces

Type	Linear form	Plot	Parameters	Adsorbent		
				A1	A2	A3
			q	2.597	3.226	2.907
Type 1	$\frac{t}{qt} = \frac{1}{k_{21}q_e^2} + \frac{1}{q}t$	$\frac{t}{q_t}$ vs. t	K_{21}	0.002	0.002	0.006
			R^2	0.999	0.998	0.998
			ARE (%)	0.99	1.04	1.10
Type 2	$\frac{1}{qt} = \frac{1}{q} + \left(\frac{1}{k_{22}q_e^2}\right)\frac{1}{t}$	$\frac{1}{q_t}$ vs. $\frac{1}{t}$	q	0.225	0.322	0.457
			K_{22}	0.368	0.250	0.159
			R^2	0993	0.996	0.993
			ARE (%)	2.21	2.19	2.40
			q	0.392	0.555	0.559
Type 3	$q_t = q - \left(\frac{1}{k_{23}q_e}\right)\frac{q_t}{t}$	q_t vs. $\frac{q_t}{t}$	K_{23}	0.050	0.026	0.028
			R^2	0.990	0.992	0.989
			ARE (%)	3.42	4.13	3.24
			q	0.533	0.546	0.536
Type 4	$\frac{qt}{t} = kq_e^2 + kq_t$	$\frac{qt}{t}$ vs. q_t	K_{24}	0.095	0.047	0.079
			R^2	0.989	0.946	0.961
			ARE (%)	3.78	2.92	3.44

Table 5 Parameters of the Elovich and the pseudo-first-order models for the removal of MB dye with MWCNT–COOH–cellulose (A1), MWCNT–COOH–cellulose with MgO directly (A2), and MWCNT–COOH–cellulose with MgO indirectly (A3) surfaces

Model	Linear form	Plot	Parameters	Adsorbent		
				A1	A2	A3
Pseudo-first-order	$\log(q_e - q_t) = \log q_e - (k_1/2.303)\, t$	$\log(q_e - q_t)$ vs. t	q	6.194	4.036	4.932
			K_1	0.051	0.053	0.055
			R^2	0.993	0.992	0.992
			ARE (%)	3.11	2.94	3.04
Elovich	$q_t = \frac{1}{\beta}\ln\alpha\beta + \frac{1}{\beta}\ln t$	q_t vs. $\ln t$	α	0.109	0.158	0.147
			β	17.54	15.15	16.67
			R^2	0.972	0.979	0.986
			ARE (%)	3.48	3.88	4.24

The linear form is presented by the following equation: [43]:

$$q_t = \frac{1}{\beta}\ln(\alpha\beta) + \frac{1}{\beta}\ln t, \tag{19}$$

where β is the Elovich constant related to the extent of surface coverage (g/mg), α is the amount of methylene blue dye adsorbed onto the MWCNT–COOH–cellulose (A1), MWCNT–COOH–cellulose with MgO directly (A2), and MWCNT–COOH–cellulose—with MgO indirectly (A3) surfaces at time t (mg g^{-1}), and α is the initial adsorption rate (mg/g min). Elovich plot of MB dye adsorption for all three nanocomposites at room temperatures is given in Fig. 16. As we can see in Table 5, α and β were determined by Elovich plot.

As listed in the kinetic study results in Tables 4 and 5, removal of methylene blue dye by MWCNT–COOH–cellulose (A1), MWCNT–COOH–cellulose with MgO directly (A2), and MWCNT–COOH–cellulose with MgO indirectly (A3) surfaces as nanocomposite adsorbents from aqueous solution was well interpreted with type (I) of pseudo-second-order model due to the high value of correlation coefficients (R^2) and low value for average relative error (ARE).

Table 6 Comparison of adsorption capacities of various adsorbents for MB dye removal

Adsorbent	Dye	q (mg/g)	Time	Temperature (K)	pH	References
Polydopamine microspheres	Methylene blue	88.89	80 (min)	298	6.5	[1]
Activated carbon	Methylene blue	270.27	5 (h)	298	6	[5]
Graphene oxide	Methylene blue	243.90	5 (h)	298	6	[5]
Carbon nanotubes	Methylene blue	188.68	5 (h)	298	6	[5]
MWCNT–SH	Methylene blue	100	60 (min)	298	6	[12]
Bamboo-based activated carbon	Methylene blue	454.20	250 (min)	303	7	[13]
Garlic peel	Methylene blue	82.64	210 (min)	303	6	[14]
$Cr(OH)_3$–NPs–CNC hybrid nanocomposite	Methylene blue	106	60 (min)	303	7	[24]
OMWCNT–Fe_3O_4	Methylene blue	1.11	60 (min)	298	6.5	[28]
OMWCNT–carrageenan–Fe_3O_4	Methylene blue	1.24	60 (min)	298	6.5	[28]
$ZnCl_2$-activated carbon	Methylene blue	274.62	90 (min)	298	6.5	[44]
Partially hydrolyzed polyacrylamide/cellulose nanocrystal	Methylene blue	170.56	240 (min)	298	6.5	[45]
Biochar/AlOOH nanocomposite	Methylene blue	85,036	–	298	–	[46]
ZnS:Cu nanoparticle-loaded on activated carbon	Methylene blue	51.70	2.2 (min)	–	7	[47]
Pyrolytic tire char	Methylene blue	65.81	–	298	7	[48]
A1	Methylene blue	109.89	55 (min)	298	–	This work
A2	Methylene blue	178.57	55 (min)	298	–	This work
A3	Methylene blue	208.33	55 (min)	298	–	This work
SA–cl–poly(AA)–TiO_2	Methylene blue	2257.36	–	298	6.8	[49]
XG/SiO_2 nanocomposite	Methylene blue	432.90	35 (min)	298	8	[50]
mwXG-g-PANi/SiO_2 nanocomposites	Methylene blue	1250	45 (min)	298	9	[51]

Conclusion

In this work, the MWCNT–COOH–cellulose (A1), MWCNT–COOH–cellulose with MgO directly (A2), and MWCNT–COOH–cellulose with MgO indirectly (A3) nanocomposites were synthesized and used for the removal of methylene blue dye from solutions. For characterization of nanocomposite surfaces, XRD and SEM methods were used. For the adsorption of methylene blue dye onto the nanocomposite adsorbent surface, 55 min was selected as the best contact time. The equilibrium and thermodynamic study of adsorption were investigated. The enthalpy (ΔH°), entropy (ΔS°), and Gibbs energy (ΔG°) were calculated; these results showed that the adsorption of MB dye onto all three nanocomposites as adsorbents can be successfully described with type (III) of Langmuir model. Also, kinetic data were fitted with type (I) of the pseudo-second-order kinetic model (Table 6).

References

1. Fu, J., Chen, Z., Wang, M., Liu, S., Zhang, J., Zhang, J., Han, R., Xu, Q.: Adsorption of methylene blue by a high-efficiency adsorbent(polydopamine microspheres): kinetics, isotherm, thermodynamics and mechanism analysis. Chem. Eng. J. **259**, 53–61 (2015)
2. El Salam, HMAbd, Zaki, T.: Removal of hazardous cationic organic dyes from water using nickel-based metal-organic frameworks. Inorg. Chim. Acta **471**, 203–210 (2018)
3. Gupta, V.K., Ali, I., Suhas, M.D.: Equilibrium uptake and sorption dynamics for the removal of a basic dye (basic red) using low-cost adsorbents. Colloid. Interface. Sci. **265**, 257–264 (2003)
4. Biopolymers for dye removal via foam separation: M. Groß M. Tupinamba Lima M. Uhlig A. Ebraheme O. Roeber B. Olschewski R. von Klitzing R. Schomäcker M. Schwarze. Sep. Purif. Technol. **188**, 451–457 (2017)
5. Li, Y., Du, Q., Liu, T., Peng, X., Wang, J., Sun, J., Wang, Y., Wu, S., Wang, Z., Xia, Y., Xia, L.: Comparative study of methylene blue dye adsorption onto activated carbon, graphene oxide, and carbon nanotubes. Chem. Eng. Res. Des. **91**, 361–368 (2013)
6. Pandey, S., Ramontja, J.: Guar gum-grafted poly(acrylonitrile)-templated silica xerogel: nanoengineered material for lead ion removal. J. Anal. Sci. Technol **7**, 24 (2016)
7. Pandey, S.: A comprehensive review on recent developments in bentonite-based materials used as adsorbents for wastewater treatment. J. Mol. Liq. **241**, 1091–1113 (2017)
8. Wojciech, K., Agnieszka, H., Walerian, A., Ewa, M.: Adsorption of cationic dyes onto Fe@graphite core–shell magnetic nanocomposite: Equilibrium, kinetics and thermodynamics. Chem ENG Res Design. **129**, 259–270 (2018)
9. Adeyemo, A.A., Adeoye, I.O., Bello, O.S.: Adsorption of dyes using different types of clay: a review. Appl. Water Sci. **7**, 543–568 (2017)
10. Sukanya, K., Ipsita, H., Chowdhury, M., Kanti, N.: Synthesis of hexagonal shaped nanoporous carbon for efficient adsorption of methyl orange dye. J Mol. Liquids. **234**, 417–423 (2017)
11. Seow, T.W., Lim, C.K.: Removal of dye by adsorption: a review. Int. J. Appl. Eng. Res. **11**(4), 2675–2679 (2016)
12. Apurva, A., Narvekar, J.B., Fernandes, S.G., Tilve, S.G.: Adsorption behavior of methylene blue on glycerol based carbon materials. J. Env Chem Eng. **6**, 1714–1725 (2018)
13. Hameed, B.H., Din, A.T.M., Ahmad, A.L.: Adsorption of methylene blue onto bamboo-based activated carbon: kinetics and equilibrium studies. J. Hazard. Mater. **141**, 819–825 (2007)
14. Hameed, B.H., Ahmad, A.A.: Batch adsorption of methylene blue from aqueous solution by garlic peel, an agricultural waste biomass. J. Hazard. Mater. **164**, 870–875 (2009)
15. Hameed, B.H., Ahmad, A.L., Latiff, K.N.A.: Adsorption of basic dye (methylene blue) onto activated carbon prepared from rattan sawdust. Dyes Pigm. **75**(1), 143–149 (2007)
16. Adewumi, O., Folahan, A., Ezekiel, O.: Liquid phase scavenging of Cd (II) and Cu (II) ions onto novel nanoscale zero-valent manganese (nZVMn): equilibrium, kinetic and thermodynamic studies. Environ. Nanotechnol. Monit. Manage. **8**, 63–72 (2017)
17. Marrakchi, F., Auta, M., Khanday, W.A., Hameed, B.H.: High-surface-area and nitrogen-rich mesoporous carbon material from fishery waste for effective adsorption of methylene blue. Powder Technol. **321**, 428–434 (2017)
18. Konicki, W., Aleksandrzak, M., Moszyński, D., Mijowska, E.: Adsorption of anionic azo-dyes from aqueous solutions onto graphene oxide: equilibrium, kinetic and thermodynamic studies. J. Colloid Interface Sci. **496**, 188–200 (2017)
19. Chen, H., Ding, J., Wang, W., Wei, X., Lu, J.: Water adsorption characteristics of MCM-41 post-modified by Al grafting and cations doping: equilibrium and kinetics study. Adsorption. **23**, 113–120 (2017)
20. Sethi, J., Farooq, M., Sain, S., Sain, M., Sirviö, J.A., Illikainen, M., Oksman, K.: Water resistant nanopapers prepared by lactic acid modified cellulose nanofibers. Cellulose **25**, 259–268 (2018)
21. Makhado, E., Pandey, S., Nomngongo, N.P., Ramontja, J.: Preparation and characterization of xanthan gum-cl-poly(acrylic acid)/o-MWCNTs hydrogel nanocomposite as highly effective re-usable adsorbent for removal of methylene blue from aqueous solutions. J. Colloid Interface Sci. **513**, 700–714 (2018)
22. Makhado, E., Pandey, S., Nomngongo, N.P., Ramontja, J.: Fast microwave-assisted green synthesis of xanthan gum grafted acrylic acid for enhanced methylene blue dye removal from aqueous solution. Carbohydr. Polym. **176**, 315–326 (2017)
23. Pandey, S., Ramontja, J.: Natural bentonite clay and its composites for dye removal: current state and future potential. Am. J. Chem. Appl. **3**(2), 8–19 (2016)
24. Nekouei, F., Nekouei, S., Keshtpour, F., Noorizadeh, H., Wang, S.: Cr(OH)3-NPs-CNC hybrid nanocomposite: a sorbent for adsorptive removal of methylene blue and malachite green from solutions. Environ. Sciand. Pollut. Res. **24**(32), 25291–25308 (2017)
25. Maneerung, T., Liew, J., Dai, Y., Kawi, S., Chong, C., Wang, C.H.: Activated carbon derived from carbon residue from biomass gasification and its application for dye adsorption: Kinetics, isotherms and thermodynamic studies. Bioresour. Technol. **200**, 350–359 (2016)
26. Babaei, A.A., Khataee, A., Ahmadpour, E., Sheydaei, M., Kakavandi, B., Alaee, Z.: Optimization of cationic dye adsorption on activated spent tea: equilibrium, kinetics, thermodynamic and artificial neural network modeling. Korean J. Chem. Eng. **33**(4), 1352–1361 (2016)

27. Van der Lee, M.K., Van Dillen, A.J., Bitter, J.H., Jong, K.P.D.: Deposition precipitation for the preparation of carbon nanofiber supported nickel catalysts. J Am Chem Soc. **127**, 13573–13582 (2005)
28. Duman, O.: TunçS, ürkanT, BaharP, BozoğlanK: Synthesis of magnetic oxidized multiwalled carbon nanotube-κ-carrageenan-Fe_3O_4nanocomposite adsorbent and its application in cationic Methylene Blue dye adsorption. Carbohydr. Polym. **147**, 79–88 (2016)
29. Srilakshmi, C., Sarafm, R.: Ag-doped hydroxyapatite as efficient adsorbent for removal of Congo red dye from aqueous solution: Synthesis, kinetic and equilibrium adsorption isotherm analysis. Microporous Mesoporous Mater. **219**, 134–144 (2016)
30. Ahmed, M.J.: Application of agricultural based activated carbons by microwave and conventional activations for basic dye adsorption: review. J. Environ. Chem. Eng. **4**(1), 89–99 (2016)
31. Putra, E.K., PranowoR, SunarsoJ, IndraswatiN, IsmadjiS: Performance of activated carbon and bentonite for adsorption of amoxicillin from wastewater: Mechanisms, isotherms and kinetics. Water Res. **43**(9), 2419–2430 (2009)
32. Tanhaei, B., Ayati, A., Lahtinen, M., Sillanpaa, M.: Preparation and characterization of a novel chitosan/Al_2O_3/magnetite nanoparticles composite adsorbent for kinetic, thermodynamic and isotherm studies of methyl orange adsorption. Chem. Eng. J. **259**, 1–10 (2015)
33. Wei, D., Li, M., Wang, X., Han, F., Li, L., Guo, J., Ai, L., Fang, L., Liu, L., Du, B., Wei, Q.: Extracellular polymeric substances for Zn (II) binding during its sorption process onto aerobic granular sludge. J. Hazard Mater. **301**, 407–415 (2016)
34. Saroyan, H.S., Giannakoudakis, D.A., Sarafidis, C.S., Lazaridis, N.K., Deliyanni, E.A.: Effective impregnation for the preparation of magnetic mesoporous carbon: application to dye adsorption. J. Chem. Technol. Biotechnol. **92**(8), 1899–1911 (2017)
35. Mahmoud, H.R., Ibrahim, S.M., El-Molla, S.A.: Textile dye removal from aqueous solutions using cheap MgO nanomaterials: Adsorption kinetics, isotherm studies and thermodynamics. Adv. Powder Technol. **27**(1), 223–231 (2016)
36. Panic, S., Guzsvány, V., Kónya, Z., Kukovecz, Á., Boskovic, G.: Kinetic, equilibrium and thermodynamic studies of thiamethoxam adsorption by multi-walled carbon nanotubes. Int. J. Environ. Sci. Technol. **14**(6), 1297–1306 (2017)
37. Chung, H.K., Kim, W.H., Park, J., Cho, J., Jeong, T.Y.: Park, P.K: Application of Langmuir and Freundlich isotherms to predict adsorbate removal efficiency or required amount of adsorbent. J. Ind. Eng. Chem. **28**, 241–246 (2015)
38. Rangabhashiyam, S., Anu, N., Giri Nandagopal, M.S., Selvaraju, N.: Relevance of isotherm models in biosorption of pollutants by agricultural byproducts. J. Environ. Chem. Eng. **2**(1), 398–414 (2014)
39. Changmai, M., Purkait, M.K.: Kinetics, equilibrium and thermodynamic study of phenol adsorption using NiFe2O4 nanoparticles aggregated on PAC. J. Water Pro. Eng. **16**, 90–97 (2017)
40. Simonin, J.P.: On the comparison of pseudo-first order and pseudo-second order rate laws in the modeling of adsorption kinetics. Chem. Eng. J. **300**, 254–263 (2016)
41. Senthilkumaar, S., Kalaamani, P., Porkodi, K., Varadarajan, P.R., Subburaam, C.V.: Adsorption of dissolved reactive red dye from aqueous phase onto activated carbon prepared from agricultural waste. Bioresour. Technol. **197**, 1618–1625 (2006)
42. Siu, P.C.C., Koong, L.F., Saleem, J., Barford, J., McKay, G.: Equilibrium and kinetics of copper ions removal from wastewater by ion exchange. Chin J Chem Eng **24**(1), 94–100 (2016)
43. Han, X., Yuan, J., Ma, X.: Adsorption of malachite green from aqueous solutions onto lotus leaf: equilibrium, kinetic, and thermodynamic studies. Desalination Water Treat. **52**, 5563–5574 (2014)
44. Pezoti Jr., O., CazettaIsis, A.L., SouzaKaren, P.A.F., Bedin Alessandro, C., Martins Tais, C., Silva Vitor, L., Almeida, C.: Adsorption studies of methylene blue onto ZnCl2-activated carbon produced from buriti shells (*Mauritiaflexuosa* L.). J. Ind. Eng. Chem. **20**(6), 4401–4407 (2014)
45. Zhou, C., Wu, Q., Lei, T., Negulescul, I.: Adsorption kinetic and equilibrium studies for methylene blue dye by partially hydrolyzed polyacrylamide/cellulose nanocrystal nanocomposite hydrogels. Chem. Eng. J. **251**, 17–24 (2014)
46. Zhang, M.: GaoB: removal of arsenic, methylene blue, and phosphate by biochar/AlOOH nanocomposite. Chem. Eng. J. **226**, 286–292 (2013)
47. Asfaram, A., Ghaedi, M., Hajati, S., Rezaeinejad, M., Goudarzi, A., Mihir Purkait, K.: Rapid removal of auramine-o and methylene blue by ZnS: Cu nanoparticles loaded on activated carbon: a response surface methodology approach. J. Taiwan Chem. Eng. **53**, 80–91 (2015)
48. MakrigianniV, GiannakasA: DeligiannakisY, KonstantinouI: Adsorption of phenol and methylene blue from aqueous solutions by pyrolytic tire char: Equilibrium and kinetic studies. J. Environ. Chem. Eng. **3**, 574–582 (2015)
49. Thakur, S., Pandey, S., Arotiba, A.O.: Development of a sodium alginate-based organic/inorganic superabsorbent composite hydrogel for adsorption of methylene blue. Carbohydr. Polym. **153**, 34–46 (2016)
50. Thakur, S., Pandey, S., Arotiba, O.A.: Sol–gel derived xanthan gum/silica nanocomposite—a highly efficient cationic dyes adsorbent in aqueous system. Int. J. Biol. Macromol. **103**, 596–604 (2017)
51. Pandey, Sadan and Fosso-Kankeu, E., Ramontja, J.: Efficient and rapid adsorption characteristics of templating xanthan gum-graft-poly(aniline) and silica nanocomposite toward removal of toxic methylene blue dyes. 9th Int'l Conference on advances in science, engineering, technology & waste management (ASETWM-17) Nov. 27–28, 2017 Parys, South Africa

Affiliations

Mohammad Sajjad Khalili[1] · Karim Zare[1] · Omid Moradi[2] · Mika Sillanpää[3]

[1] Department of Chemistry, Science and Research Branch, Islamic Azad University, Tehran, Iran

[2] Department of Chemistry, Shahr-e-Qods Branch, Islamic Azad University, Tehran, Iran

[3] Department of Green Chemistry, Lappeenranta University of Technology, Sammonkatu 12, 50130 Mikkeli, Finland